Hsp70 gene association with nuclear speckles is Hsp70 promoter specific

Yan Hu, Matt Plutz, and Andrew S. Belmont

Department of Cell and Developmental Biology, University of Illinois, Urbana, IL 61801

Many mammalian genes localize near nuclear speckles, nuclear bodies enriched in ribonucleic acid–processing factors. In this paper, we dissect cis-elements required for nuclear speckle association of the heat shock protein 70 (Hsp70) locus. We show that speckle association is a general property of Hsp70 bacterial artificial chromosome transgenes, independent of the chromosome integration site, and can be recapitulated using a 2.8-kilobase HSPA1A gene fragment. Association of Hsp70 transgenes and their transcripts with nuclear speckles is transcription dependent, independent of the transcribed sequence identity, but dependent on the Hsp70 promoter sequence. Transgene speckle association does not correlate with the amount of transcript accumulation, with large transgene arrays driven by different promoters showing no speckle association, but smaller Hsp70 transgene arrays with lower transcript accumulation showing high speckle association. Moreover, despite similar levels of transcript accumulation, Hsp70 transgene speckle association is observed after heat shock but not cadmium treatment. We suggest that certain promoters may direct specific chromatin and/or transcript ribonucleoprotein modifications, leading to nuclear speckle association.

Introduction

The eukaryotic nucleus is a complex, dynamic structure partitioned into chromosome territories and various interchromatin compartments (Cremer and Cremer, 2001). One of the first distinct nuclear bodies described within the interchromatin compartment were nuclear speckles, present in nuclei from a wide range of species. Also described as SC-35–staining domains (Wansink et al., 1993) or interchromatin granule clusters (Thiry, 1995), these proteinaceous nuclear bodies are enriched in proteins involved in RNA-processing events, including transcription, splicing, and nuclear export (Mintz et al., 1999; Hall et al., 2006).

The function of nuclear speckles is still debated. Most transcription and splicing takes place away from these speckles (Fakan and Nobis, 1978; Cmarko et al., 1999), and one leading model suggests speckles serve primarily as storage sites for RNA-processing components (Spector et al., 1983; O'Keefe et al., 1994). This model of speckles as relatively inactive, "passive" depositories of RNA-processing components has been challenged by more recent demonstrations that a subset of active genes are preferentially localized to the periphery of nuclear speckles (Xing et al., 1995; Smith et al., 1999; Shopland et al., 2003).

Of the handful of gene loci examined by DNA and RNA FISH, two distinct classes were described (Smith et al., 1999). Genes in both classes localize to the speckle periphery, but transcripts of class 1 genes show accumulations within the speckle interior, whereas transcripts of class 2 genes remain outside of the speckles. For class 1 genes, entry and exit of nascent RNA into the adjacent speckle may be related to different steps of RNA processing and nuclear transport (Holt et al., 2007; Smith et al., 2007).

Dissection of the physiological function of nuclear speckles likely will require identification of cis- and trans-factors that control whether a particular gene is associated with nuclear speckles and whether the transcripts of these speckle-associated genes transit through the speckle interior. To date, studies have largely focused on speckle association of particular endogenous gene or chromosome loci.

Recently, we showed that of three CHO cell lines containing dihydrofolate reductase (DHFR), metallothionein (MT), or

Correspondence to Andrew S. Belmont: asbel@illinois.edu

Abbreviations used in this paper: BAC, bacterial artificial chromosome; CMF-PBS, calcium- and magnesium-free PBS; DEPC, diethylpyrocarbonate; DHFR, dihydrofolate reductase; Hsp70, heat shock protein 70; MT, metallothionein; PTS, peroxisome-targeting sequence.

The Rockefeller University Press $30.00
J. Cell Biol. Vol. 191 No. 4 711–719
www.jcb.org/cgi/doi/10.1083/jcb.201004041

heat shock protein 70 (Hsp70) bacterial artificial chromosome (BAC) transgenes, only the Hsp70 BAC transgene associated specifically with nuclear speckles after transcriptional induction, recapitulating the behavior of the native Hsp70 gene locus (Jolly et al., 1999). In this cell line, the tandem array of Hsp70 BAC transgenes behaved as class 1 genes, with the transgenes localizing to the speckle periphery and the Hsp70 transcript accumulating within the speckles at later times after heat shock (Hu et al., 2009). Here, we apply this Hsp70 transgene system to dissect the cis-elements required for gene-specific speckle association.

Results and discussion

Association with nuclear speckle is specific for Hsp70 BAC

In our previous work, we analyzed four cell lines, each with a different BAC transgene array containing an inducible housekeeping gene (Fig. 1 A): human Hsp70 BAC 92G8 (180.5 kb), human MT BAC 134B2 (173 kb), mouse DHFR BAC 057L22 (175.5 kb), and mouse DHFR BAC 560M7 (122 kb; not depicted). The Hsp70 BAC contains three Hsp70 genes with high sequence homology, HPA1A, HPA1L, and HPA1B, within a 10-kb region. Only the cell line containing the Hsp70 BAC showed high levels of association of the BAC transgene array with nuclear speckles.

To verify that this nuclear speckle association was indeed specific for the Hsp70 BAC transgene rather than the BAC chromosome integration site, we repeated these experiments with multiple, independent stable cell clones containing Hsp70, MT, and DHFR (057L22) BAC arrays. Tn5 transposition was used to randomly insert a 10-kb, 256-mer lac operator repeat together with a selectable marker into these BACs (Hu et al., 2009). We then transfected these BACs into DHFR$^{-/-}$ CHO DG44 cells stably expressing an EGFP-dimer lac repressor–NLS fusion protein (EGFP-LacI) and selected independent stable clones with varying BAC copy number and chromosome integration sites (Fig. 1 B).

All five cell clones containing the Hsp70 BAC showed significantly higher speckle associations (40–55%), even without heat shock, than any of the cell clones carrying the DHFR or MT BACs (10–25%), with or without gene induction (Fig. 1 C and Table S1). We defined the speckle association index as the percentage of GFP-LacI signals that by light microscopy were touching the edge of SC-35–immunostained nuclear speckles. After heat shock, all cell clones with the Hsp70 BAC showed significant ($P < 0.01$) increases (15–40%) in transgene speckle association, yielding association indexes ranging from 65 to 86% (Fig. 1 C). None of the four cell clones containing the DHFR BAC or three cell clones containing the MT BAC showed a significant increase in speckle association after gene induction (Fig. 1 C and Table S1), verifying the sequence specificity for BAC transgene nuclear speckle association.

In comparison, the endogenous Hsp70 locus in human primary fibroblasts showed an increase in speckle association from 10 to 90% after heat shock (Jolly et al., 1999). Why the BAC Hsp70 transgenes show a higher speckle association in the absence of heat shock is not clear. Insertion of multiple BAC copies may create a gene-rich, constitutively active chromatin domain caused by the presence of multiple housekeeping genes on the BAC. RNA FISH using the entire BAC as a probe revealed a detectable signal before heat shock, but this signal did not colocalize within adjacent nuclear speckles or show any particular localization relative to adjacent nuclear speckles (Fig. S1, B and C). Alternatively, the increased speckle association without heat shock might reflect increased Hsp70 gene dosage and level of constitutive Hsp70 gene expression. As we later show, an Hsp70 BAC with only one Hsp70 gene shows low speckle association without heat shock.

2.8-kb fragment containing the HSPA1A gene is sufficient for nuclear speckle association and localization of HSPA1A RNA inside speckle

To test whether flanking sequences on the Hsp70 BAC were required for speckle association, we transfected a plasmid (Fig. 2 A) containing a 2.8-kb fragment, comprised of the HSPA1A transcribed gene sequence plus 330 bp of upstream regulatory sequence, and a 64-mer lac operator repeat into CHO DG44 cells expressing EGFP-LacI. Examination of clone pSP14_4_B4 showed that the 2.8-kb DNA fragment encompassing the HSPA1A gene was sufficient to recapitulate both the speckle association and the transcript accumulation within the speckle at later times (20–30 min) after heat shock (Fig. 2 B), as previously observed for the entire Hsp70 BAC (Fig. 1 B; Hu et al., 2009).

Speckle association of plasmids carrying the 2.8-kb HSPA1A fragment is largely independent of the chromosome integration site. All six independent stable cell clones selected containing plasmid transgene arrays showed statistically significant increases ($P < 0.05$) in transgene array speckle association after heat shock, with four out of six clones showing significant increases of >30% after heat shock ($P < 0.0001$; Fig. 2 C and Table S1). Clone pSP14_4_C5 had a very high (85%) association index without heat shock that increased to near 100% after heat shock.

The HSPA1A transgene association with nuclear speckles is promoter dependent

Replacing the HSPA1A promoter with the MT2A promoter, we repeated the previous experiments. None of the five stable cell clones analyzed showed significant increases in speckle association after zinc addition, although RNA FISH confirmed HSPA1A expression after zinc induction in all clones (Fig. 3 A and Table S1). We next constructed a plasmid containing the MT2A gene under the control of the HSPA1A promoter. RNA FISH confirmed MT2A transgene expression after heat shock in four stable cell clones carrying this plasmid construct (Fig. 3 B). Significant ($P < 0.01$) increases in transgene nuclear speckle association after heat shock (Fig. 3 B and Table S1) and localization of MT2A transcripts to the nuclear speckle interior (Fig. 3 C) were observed in all four clones. These experiments demonstrated that nuclear speckle association is HSPA1A promoter dependent and independent of whether the HSPA1A or MT2A transcript was expressed.

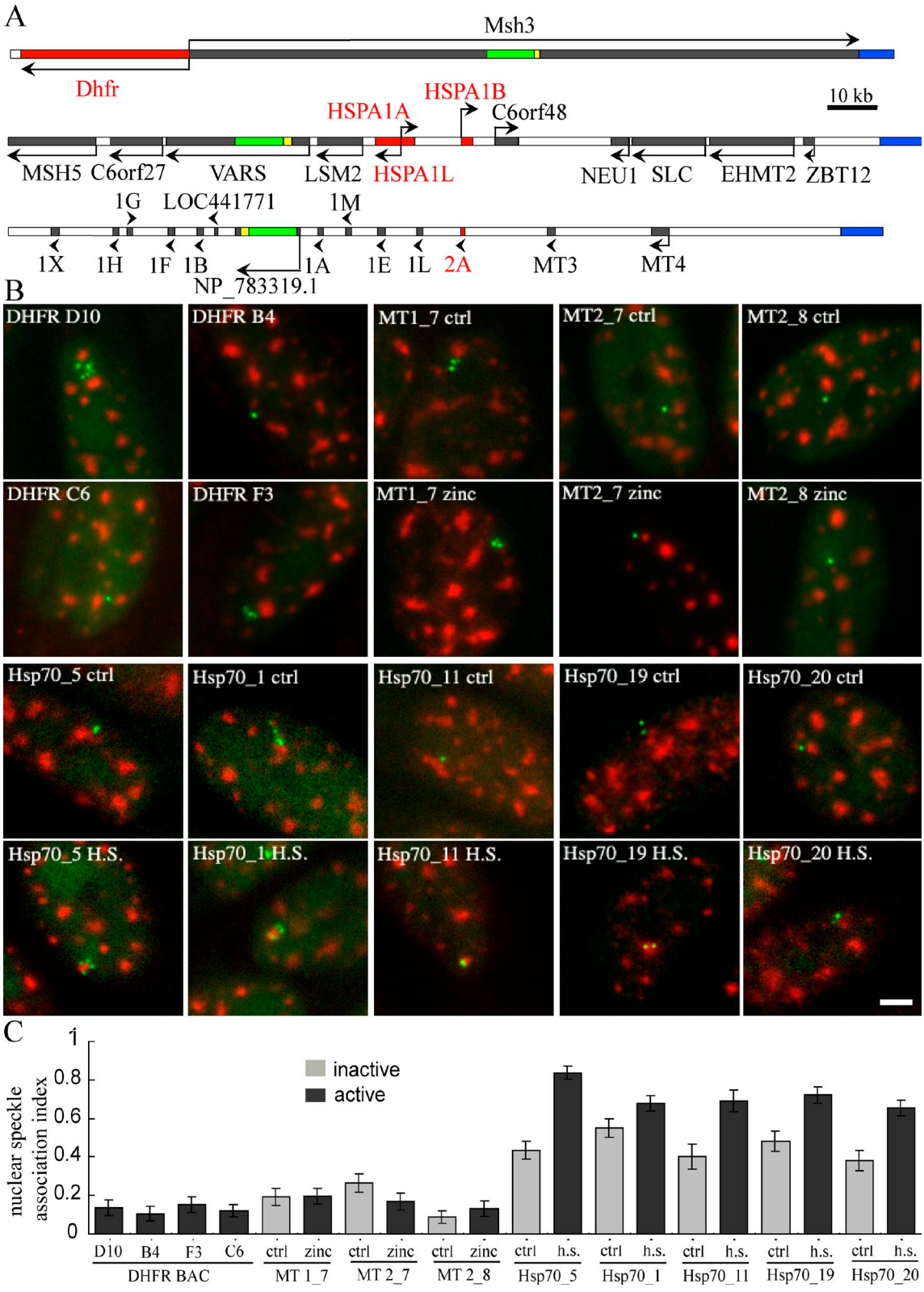

Figure 1. **Transgene nuclear speckle association is specific for Hsp70 BAC.** (A) BAC constructs (top to bottom): DHFR 057L22-K-8.32-C-29, Hsp70 92G8-K/N-8.32-C-2, and MT 134B2-K/N-8.32-C-8. Inducible genes whose expression we monitored (red), other genes (gray), transposable elements carrying lac operator repeats (green) and selectable markers (yellow), and vector backbones (blue) are shown in linear form. Arrows show transcription units. (B) Transgenes labeled with EGFP-LacI (green) showed no obvious association with nuclear speckles immunostained with SC-35 antibody (red) in four DHFR BAC and three MT BAC cell lines before (control [ctrl], top) and after (zinc, second row) zinc induction. All five Hsp70 cell lines showed increased nuclear speckle association 30 min after heat shock (H.S., bottom) relative to before heat shock (ctrl, third row). Optical sections are shown without deconvolution. Bar, 2 μm. (C) Nuclear speckle association for all BAC cell lines. DHFR and MT BAC cell lines showed a low background level of ~10–20% speckle association. All Hsp70 BAC cell lines showed ~40% elevated speckle associations before heat shock that increased significantly ($P < 0.01$) after heat shock. Error bars represent SEM.

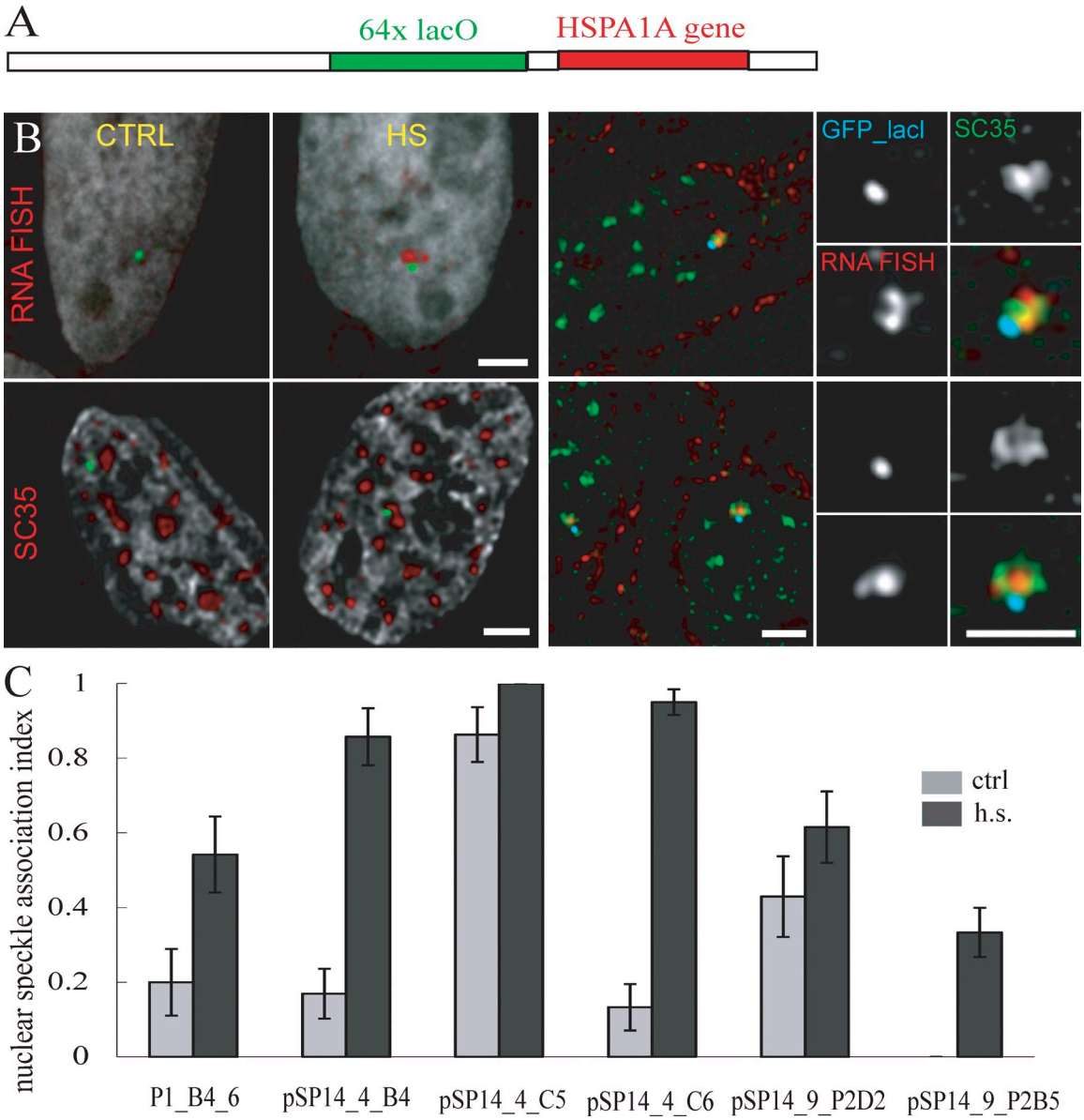

Figure 2. **2.8-kb HSPA1A fragment is sufficient for nuclear speckle association.** (A) Plasmid pSP14-14 contains the 2.8-kb HSPA1A gene and a 64-mer lac operator repeat. (B) RNA FISH and SC-35 immunostaining for pSP14_4_B4 CHO DG44 cell clone containing HSPA1A plasmid transgenes. (left) Nuclear DNA counterstained with DAPI (gray) and EGFP-LacI (green). Top two panels show HSPA1A RNA FISH signals (red) before (left) and after (right) heat shock. Images are shown without deconvolution. Bottom two panels show SC-35 staining (red) before (left) and after (right) heat shock. (right) Examples of RNA FISH combined with SC-35 immunostaining: EGFP-LacI (blue), SC-35 staining (green), and RNA FISH signals (red). Transgene arrays are shown at a higher magnification on the right. Bars, 2 µm. (C) Nuclear speckle association indexes for six independently derived cell clones. ctrl, control. h.s., 30 min after heat shock. Error bars show SEM.

Transcription is required for nuclear speckle association

To test whether transcription might be required for speckle association, we measured speckle association after inhibition of transcription by α-amanitin. α-Amanitin specifically inhibits the RNA polymerase II largest subunit and targets it for degradation (Nguyen et al., 1996). To facilitate statistical analysis, we used the HSPA1A plasmid cell line (pSP14-4-B4), which showed the largest change in nuclear speckle association before and after heat shock. As reported previously (Lallena and Correas, 1997), α-amanitin led to a reduction in nuclear speckle number and increase in speckle roundness (Fig. 4 A). α-Amanitin treatment for 4 h before heat shock, at concentrations previously shown to result in near-complete degradation of the largest subunit of RNA polymerase II (Nguyen et al., 1996), completely blocked nuclear speckle association of the HSPA1A transgene array after heat shock (Fig. 4 B). We conclude that increased nuclear speckle association of the HSP1A1 gene after heat shock requires transcription.

The HSPA1A transgene nuclear speckle association does not correlate with the level of nascent transcript accumulation

One explanation for promoter specificity and the requirement for transcription would be if association of gene loci with nuclear

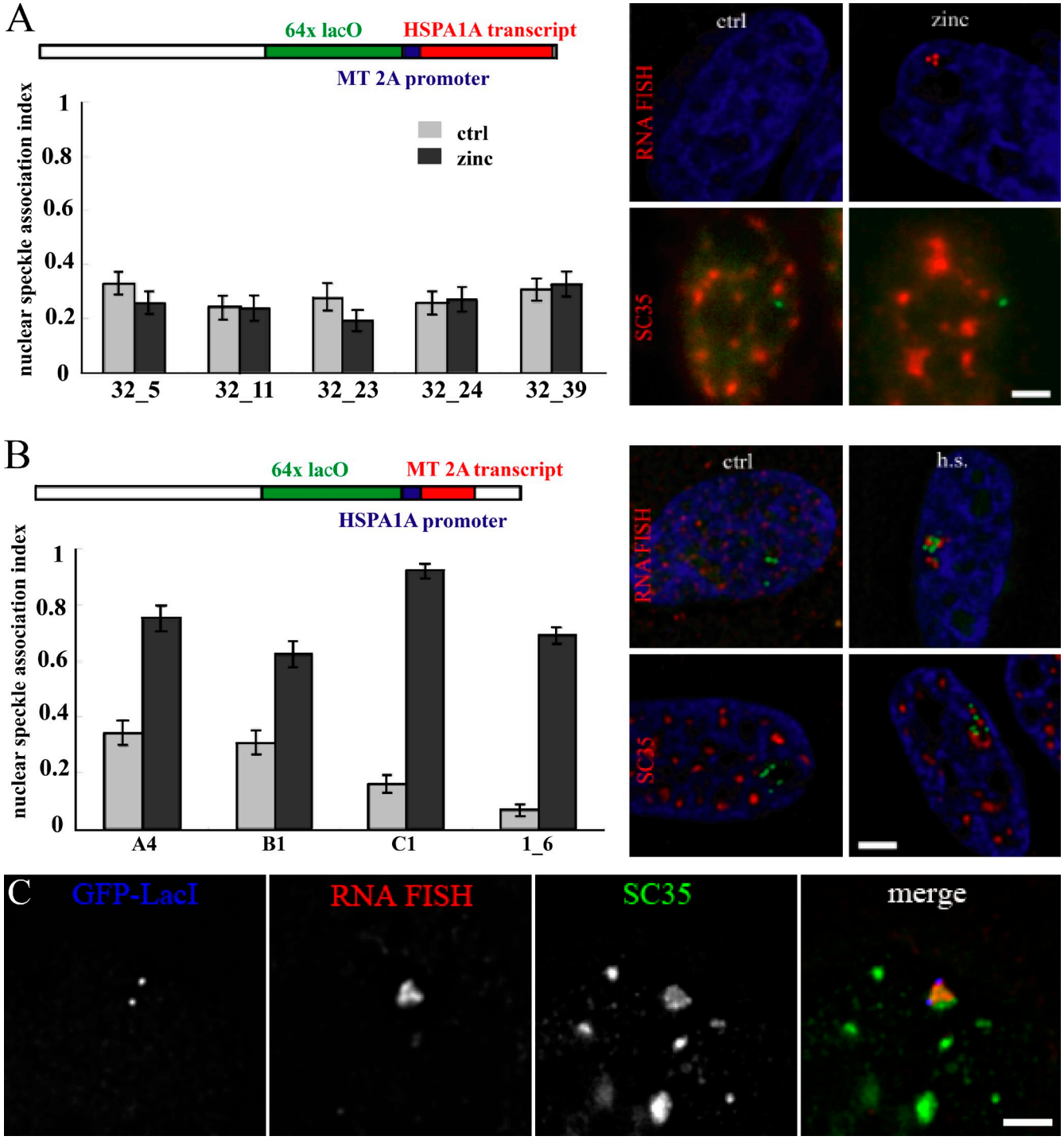

Figure 3. **The HSPA1A transgene association with nuclear speckles is promoter dependent.** (A, top left) Plasmid pSP14-MT2A + HSPA1A containing the MT2A promoter driving the HSPA1A gene and a 64-mer lac operator repeat. (bottom left) Transgene nuclear speckle association indexes for five independent cell clones before (ctrl) or after zinc induction. (right, top row) RNA FISH (red) before (left) and after (right) zinc induction; DAPI DNA counterstaining (blue). (right, bottom row) SC-35 staining (red) before (left) and after (right) zinc induction. (B) The corresponding layout as in A, but for plasmid pSP14-HSPpro + MT2A containing the HSPA1A promoter driving the MT2A gene. (C) Combined RNA FISH SC-35 immunostaining for cell clone pSP14-HSPpro + MT2A_C1. Transgenes were labeled with EGFP-LacI (left), RNA FISH signal (second from left), SC-35 staining (second from right), and merged image (right). Bars, 2 µm. Error bars show SEM.

speckles were simply dependent on the amount of accumulated nascent transcript. We used RNA FISH to estimate levels of nascent transcripts localized near the transgenes in different cell lines containing either BAC or plasmid transgene arrays that showed a wide range of transgene copy number and overall expression levels.

Using BAC recombineering, we deleted two of the three Hsp70 genes on the Hsp70 BAC. After stable transfection, we deliberately chose cell clones with low copy number insertions of this BAC as inferred by a single, low intensity GFP-labeled spot. Based on previous work (Hu et al., 2009), we estimate that

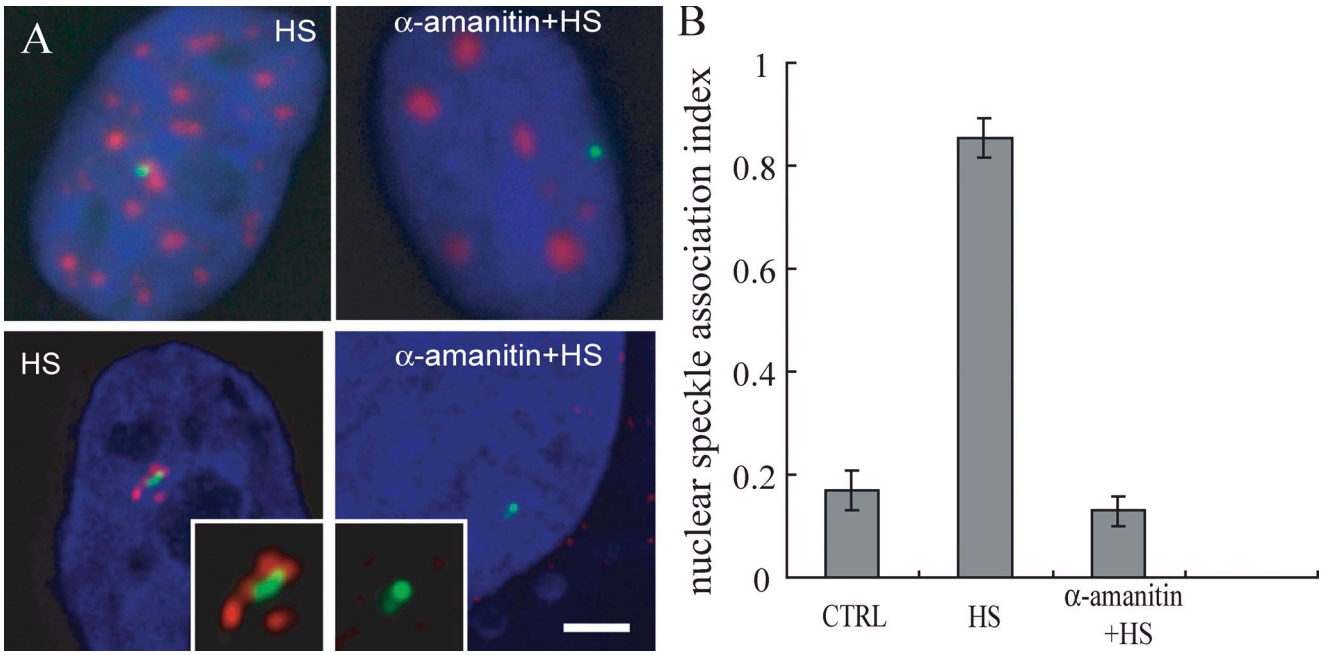

Figure 4. **Transcription is required for nuclear speckle association.** 30-min heat shock experiments using pSP14_4_B4 cells. Insets show enlarged regions containing the transgene array. (A) DAPI DNA staining is shown in blue, and EGFP-LacI is shown in green. (top) SC-35 staining (red) after heat shock (HS; left) or after heat shock with prior transcriptional inhibition with α-amanitin (right). (bottom) RNA FISH using HSPA1A probe (red) after heat shock (left) or α-amanitin treatment for 3.5 h before 30-min heat shock (right). (B) Nuclear speckle association indexes with or without transcriptional inhibitors. Bar, 2 µm. Error bars show SEM.

these cell clones contain just one to three copies of integrated BAC copies. After heat shock, these BAC transgenes showed only a small RNA FISH signal (Fig. 5, A and C), but speckle association (Fig. 5 B) was comparable with cell lines carrying the wild-type Hsp70 BAC at several times the BAC copy number (Fig. 1 C) or with cells with the HspA1A plasmid transgenes present at a high copy number (Fig. 2 C).

Using deconvolved 3D optical datasets, we made projections of the RNA FISH images for several nuclei and compared the integrated Hsp70 RNA FISH signals and mean RNA FISH intensities adjacent to the Hsp70 transgenes in different cell lines. RNA FISH was performed in parallel on different cell clones using the same probe. A duplicate set of coverslips was immunostained for SC-35 to measure speckle association.

For the two cell clones analyzed carrying the Hsp70 BAC with one Hsp70 gene, the integrated FISH signal after heat shock was approximately sixfold lower than in the MTpro_HSPA1A_32_24 plasmid transgene array expressing the HSPA1A transcript from the MT promoter after zinc induction, which showed low speckle association (Fig. 5 D). In turn, the integrated RNA FISH signal for this MTpro_HSPA1A_32_24 transgene array after zinc induction was comparable with the integrated RNA FISH signal from the HSPA1A 4_B4 plasmid transgene array showing 86% speckle association (Fig. 5 D) after heat shock. The mean intensity of the RNA FISH signal from the BAC transgene arrays was slightly lower or comparable with the mean RNA FISH signals from the plasmid transgene arrays examined, regardless of whether they showed high or low speckle association (Fig. 5 E). Therefore, the amount of nascent transcript concentration within a microscopic nuclear subvolume does not correlate with nuclear speckle gene association.

Hsp70 transgene activated by cadmium does not lead to a large increase in transgene nuclear speckle association

The Hsp70 gene can be induced by alternative stress conditions to similar levels of transcription as produced by heat shock (Williams and Morimoto, 1990). Alternative stress conditions may invoke a different promoter response than does heat shock.

Treatment of pSP14_4_B4 cells with 30 µM cadmium sulfate for 4 h resulted in an approximately threefold higher Hsp70 nascent transcript accumulation relative to that observed after heat shock (Fig. 5 D and Table S1), consistent with a previous study (Williams and Morimoto, 1990). Cadmium treatment also produced a noticeable decrease in the number of nuclear speckles, with individual speckles becoming larger and rounder (Fig. S2), although gene array experiments indicate limited changes in gene expression after cadmium treatment (Ohba et al., 2007; Kawata et al., 2009).

However, cadmium treatment resulted in only a small increase in nuclear speckle association (from 17 to 21%; $P = 0.047$), in contrast with the dramatic increase in speckle association (17–85%; $P < 0.0001$) observed in control pSP14_4_B4 cells 30 min after heat shock (Fig. S2 C and Table S1). We still observed a strong increase (17–49%; $P < 0.0001$) in nuclear speckle association with the HSP1A1 transgene array after combining the cadmium plus heat shock induction protocol (Fig. S2, B and C; and Table S1).

Cell clones containing low copy integrations of the Hsp70 BAC with a single Hsp70 gene showed an ∼26-fold lower integrated RNA FISH signal ($P < 0.0001$) than the RNA FISH signal observed for the 4_B4 plasmid HspA1A transgene array

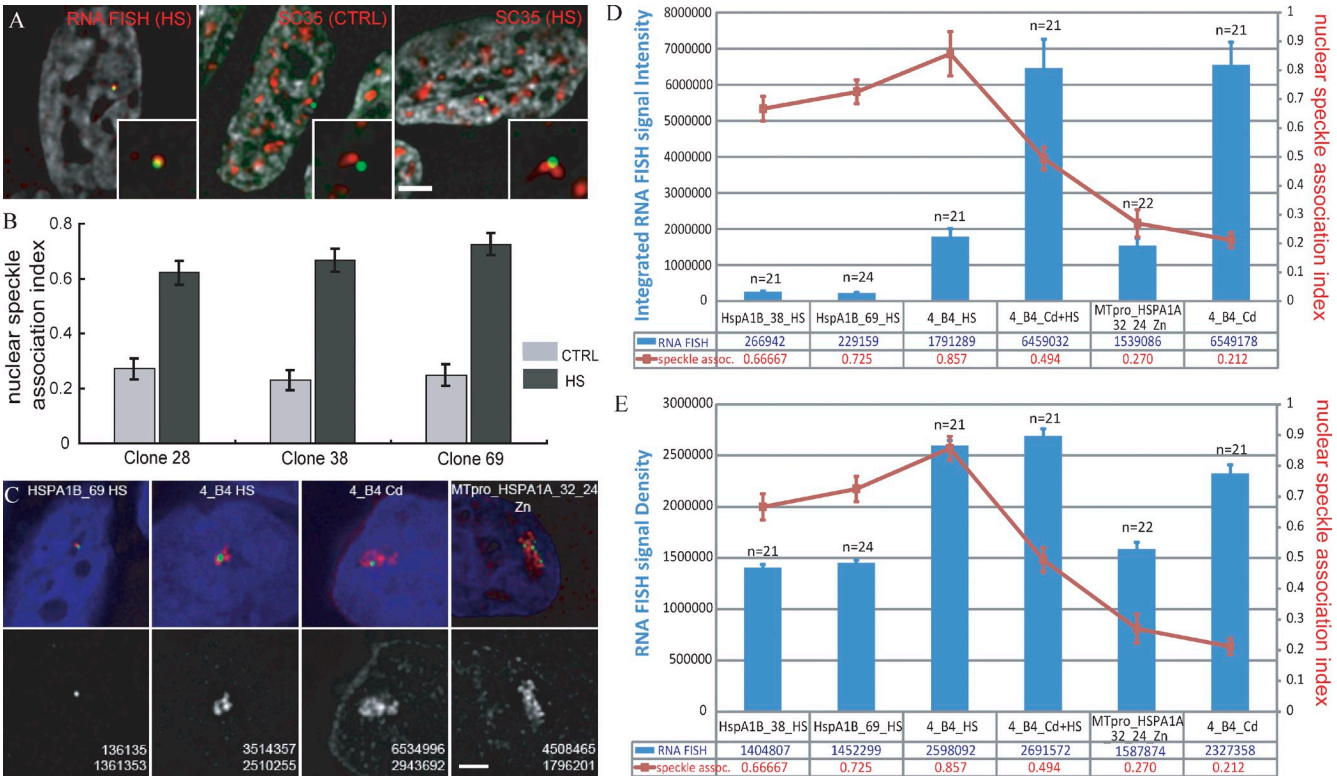

Figure 5. **The HSPA1A transgene nuclear speckle association does not correlate with levels of accumulated nascent transcripts.** (A) Low copy integration of Hsp70 BAC recombineered to contain just one Hsp70 gene still shows speckle association despite small RNA FISH signal. RNA FISH (left, red) and SC-35 immunostaining (middle and right, red) for cell clone 69 containing 92G8_HSPA1B BAC. EGFP-LacI staining is shown in green, and DAPI DNA counterstaining is shown in gray. (left) After heat shock. (middle) No heat shock. (right) 30-min heat shock. (B) Nuclear speckle association indexes for three independent stable cell clones containing low copy integrations of the 92G8_HSPA1B BAC before (CTRL) and after (HS) heat shock. (C) RNA FISH of different cell lines, scaled uniformly, after gene activation. All hybridizations used the same HSPA1A probe and were performed in parallel. Top panel shows merged images of RNA FISH (red), EGFP-LacI (green), and DAPI (blue). Bottom panel shows RNA FISH signal only. Comparisons are between cell lines HSPA1B_69 (left) containing low copy integration of the Hsp70 BAC with one Hsp70 gene, pSP14_4_B4, with an HSPA1A plasmid array after heat shock (middle left) or cadmium (middle right) induction, and MTpro_HSPA1A_32_24 containing a plasmid array with the MT promoter driving a HSPA1A transcript after zinc addition (right). Numbers in bottom right corners are the integrated RNA FISH signal (top) or the RNA FISH mean intensity (bottom) per square micrometer. (D and E) Statistical analysis of the integrated RNA FISH signal intensities (D) or mean intensities per square micrometer (blue bars, E) versus nuclear speckle association indexes (red lines) for different cell lines under different transcription induction conditions as indicated in the figure. The cell line and induction conditions are indicated on the x axis: HspA1B_38_HS, HspA1B_69_HS, two clones of Hsp70 BAC with one Hsp70 gene after heat shock, pSP14_4_B4 after heat shock (4_B4_HS), pSP14_4_B4 after heat shock plus cadmium (4_B4_CD + HS), MTpro_HSPA1A_32_24 clone after zinc induction (MTpro_HSPA1A_32_24_Zn), and pSP14_4B4 after cadmium (4B4_Cd). Numbers shown below the table in blue are means for the integrated RNA FISH signal intensities (D) or mean intensities (E), and those shown in red are speckle association indexes. Bars, 2 μm. Cell numbers (*n*) are shown for each data point. Error bars represent SEM.

after cadmium induction and a lower mean RNA FISH intensity ($P < 0.0001$; Fig. 5, D and E; and Table S1). We conclude that the HSPA1A promoter–directed increase in nuclear speckle association after transcriptional activation is specific for heat shock versus cadmium Hsp70 gene induction and is not related simply to the amount of accumulated nascent transcript produced by heat shock versus cadmium induction.

Future directions

We have demonstrated that association of an Hsp70 BAC transgene is intrinsic to the DNA sequences contained within the BAC and independent of its chromosome integration site. Moreover, just a 330-bp HSPA1A gene promoter was sufficient to reproduce both speckle association and association of heat shock or MT transcripts with the adjacent speckle after heat shock.

One possible scenario would be that the critical initiation event for speckle association corresponds to buildup of a critical threshold of nascent transcripts. Our data, though, show no correlation between transgene nuclear speckle association and the microscopic amount of nascent transcript accumulation from these transgenes, arguing against a simple threshold model. We cannot exclude the possibility that it is the local rather than microscopic transcript concentration, for instance on the gene template, that determines speckle association. However, our current working model is that the promoter of a class I gene directs a different RNA-processing machinery to the nascent transcript, resulting in a quantitatively different RNP assembly of the nascent transcript, which in turn determines speckle association.

Future experiments will be aimed at testing this model. Live-cell imaging should allow direct examination of the temporal relationship between increased transcription, accumulation of nascent transcript, and speckle formation and/or association, whereas promoter dissection will test whether the transcriptional activity of the promoter can be separated from its ability to associate with nuclear speckles.

Materials and methods

BAC constructs and BAC transgene cell lines

DHFR BAC clone 057L22 was obtained from the California Institute of Technology BAC (CITB) mouse library and is based on the pBeloBac11 vector; Hsp70 BAC clone 92G8 and MT BAC clone 134B2 were obtained from the Roswell Park Cancer Institute 11 human library and are based on the pBACe3.6 vector. The Hsp70, MT, and DHFR BACs were retrofitted to contain lac operator repeats and selectable markers as described previously (Hu et al., 2009). Circular BACs were transfected into DHFR minus CHO DG44 cells expressing EGFP-dimer LacI (clone 7) cells using Fugene 6 (Roche) according to the manufacturer's instructions. Stable cell clones containing the DHFR BAC were selected in Ham's F12 media without hypoxanthine and thymidine (Invitrogen) supplemented with 10% dialyzed FBS (Hyclone). Stable cell lines containing the Hsp70 and MT BACs were selected in 200 µg/ml G418 in Ham's F12 media supplemented with 10% FBS. Subcloning was performed using serial dilution; stable subclones were screened by light microscopy based on the presence and number of EGFP-dimer LacI nuclear spots.

Plasmid constructs

The 7.7-kb plasmid pSP14-pur + ECFP–peroxisome-targeting sequence (PTS) + 64lacO contains a puromycin-selectable marker, an ECFP-peroxisome–targeting signal, and a 64-mer lac operator repeat (Nye, 2003). We used primers forward, 5′-ATTAAAAGCCCAGCGCCGACC-3′, and reverse, 5′-CCTATGCAGACCCTACTGACC-3′, to amplify the entire 2.8-kb HSPA1A gene together with the HSPA1A promoter on the human Hsp70 BAC 92G8 (Hu et al., 2009), inserted them into the AscI site of pSP14-pur + ECFP-PTS + 64lacO, and produced plasmid pSP14-14. Next, we cut pSP14-14 with NheI to keep the HSPA1A promoter but remove the HSPA1A gene. Using PCR with primers forward, 5′-ACTCGTCCCGGCTCTTTCTA-3′, and reverse, 5′-AAGGCATATAAAGGAAACCAGAGA-3′, we amplified the MT2A gene without its promoter from human MT BAC 134B2. We inserted the PCR product into NheI-digested pSP14-14, thereby replacing the HSPA1A gene with the MT2A gene to create plasmid pSP14-HSPpro + MT2A. To replace the HSPA1A promoter with the MT2A promoter, we digested pSP14-pur + ECFP-PTS + 64lacO with NotI, removing ECFP-PTS, and religated to create pSP14-pur + 64lacO. Primers used for amplifying the MT2A promoter were forward, 5′-CCAGCACCCGGTACACTG-3′, and reverse, 5′-ACTTGGAGGAGGCGTGGT-3′. Primers used for amplifying the HSPA1A gene were forward, 5′-CTGCTGCGACAGTCCACT-3′, and reverse, 5′-CCTATGCAGACCCTACTG-3′. We linked these two fragments through the PmeI site, inserting the fusion fragment into the AscI and NotI sites of plasmid pSP14-pur + 64lacO to create plasmid pSP14-MTpro + HSPA1A.

Establishment of plasmid cell lines

The aforementioned plasmids were transfected into CHO DG44 cells expressing EGFP-dimer LacI (clone 7) cells using Lipofectamine 2000 (Invitrogen) according to the manufacturer's directions. Selection was performed in F12 media containing 7.5 µg/ml puromycin (EMD). Stable transformants were cloned by serial dilution and screened by light microscopy. PCR identified clones in which the transgenes remained intact after plasmid integration into chromosomal sites.

Heat shock and zinc induction

Standard heat shock conditions were used at 42°C for 30 min. For zinc induction of the MT BAC cell clones and cell clones with the MT2A promoter driving the HSPA1A transcript, cells were incubated in 100 µM $ZnCl_2$ at 37°C for 2 h.

Antibodies and immunofluorescence

Cells grown on coverslips were fixed in 1.6% formaldehyde in PBS* (calcium- and magnesium-free PBS [CMF-PBS] plus 0.1 mM EDTA and 5 mM $MgCl_2$) for 15 min at RT and then were permeabilized in PBS* using 0.1% Triton X-100 (Thermo Fisher Scientific) for 5 min. Cells were blocked in 5% normal goat serum (Sigma-Aldrich)/PBS* for 1 h at RT followed by incubating with primary antibodies (mouse anti-ASF/SF2 [1:200; Invitrogen] or anti–SC-35 [1:200; Sigma-Aldrich]) in 5% normal goat serum/0.1% Triton X-100/PBS* at 4°C overnight and secondary antibody (goat anti–mouse [1:1,000; Texas red])/0.1% Triton X-100/PBS* for 4 h at RT. Cells were mounted in an antifade medium containing 0.3 µg/ml DAPI (Sigma-Aldrich)/10% wt/vol Mowiol 4–88 (EMD)/1% wt/vol DABCO (Sigma-Aldrich)/25% glycerol/0.1 M Tris, pH 8.5. Optical sectioning and deconvolution were performed on a wide-field deconvolution microscope system as previously described (Tumbar et al., 1999).

RNA FISH and RNA immuno-FISH

For RNA FISH probes, the human HSPA1A gene product was PCR amplified (forward: 5′-TGATTGGCTCAGAAGGGAAA-3′; and reverse: 5′-GACCCTACTGACCCCCAAAT-3′), and the human MT2A gene product was also PCR amplified (forward: 5′-ACTCGTCCCGGCTCTTTCTA-3′; and reverse: 5′-AAGGCATATAAAGGAAACCAGAGA-3′). The HSPA1A 5′ 919-bp sequence was amplified using primers (forward: 5′-CTGCTGCGACAGTCCACTAC-3′; and reverse: 5′-GAAGTGGTTCACCAGCCTGT-3′), and the HSPA1A 3′ 960-bp sequence was amplified using primers (forward: 5′-AAGCAGACGCAGATCTTCAC-3′; and reverse: 5′-GACCCTACTGACCCCCAAAT-3′). For BAC hybridization, we used the entire Hsp70 or MT BAC. The aforementioned DNA probes for RNA FISH were biotin labeled by nick translation (BioNick kit; Invitrogen) according to the manufacturer's instructions.

RNA FISH and RNA FISH combined with immunostaining procedures were performed as previously described (Chaumeil et al., 2003). Cells grown on coverslips were washed briefly in 0.1% diethylpyrocarbonate (DEPC, $C_6H_{10}O_5$; Sigma-Aldrich)-treated CMF-PBS, fixed in freshly prepared 3% paraformaldehyde (Sigma-Aldrich), prepared using DEPC-treated CMF-PBS for 10 min at RT, and washed three times in CMF-PBS. Subsequently, cells were permeabilized in 0.5% Triton X-100/2 mM ribonucleoside–vanadyl complex (New England Biolabs, Inc.)/DEPC-treated CMF-PBS on ice for 5 min followed by blocking in 3% BSA/0.05% Tween 20/DEPC-treated CMF-PBS. Cells were incubated with primary antibody (SC-35, 1:100) at RT for 2 h followed by secondary antibody (goat anti–mouse–Alexa Fluor 350, 1:100) at RT for 2 h in the same blocking buffer with a 0.4-unit/µl RNase inhibitor (Thermo Fisher Scientific). After washing three times in DEPC-treated CMF-PBS, cells were fixed again in freshly prepared 3% paraformaldehyde in DEPC-treated CMF-PBS at RT for 10 min, washed three times in DEPC-treated CMF-PBS, and incubated in 50% formamide/2× SSC for 5 min. After hybridization, as previously described (Hu et al., 2009), the DNA probes were detected with streptavidin–Alexa Fluor 594 (Invitrogen), and coverslips were mounted in DAPI-free antifade mounting medium. The aforementioned procedure was for RNA immuno-FISH; RNA FISH alone was performed without the prior immunostaining procedure.

Transcription inhibition and cadmium treatment

Transcription in HSPA1A plasmid transgene cell lines was inhibited by incubating cells in 100 µg/ml α-amanitin (Sigma-Aldrich) for 3.5 h before 42°C heat shock treatment for 30 min. For cadmium induction of heat shock genes, 30 µM cadmium sulfate (Sigma-Aldrich) was added to cells at 37°C for 4 h. For combined cadmium and heat shock induction, cadmium was added to cells for 3.5 h, and then cells were moved to 42°C for an additional 30 min before fixation.

BAC homologous recombination

The 8-kb DNA sequences including the HSPA1A and HSPA1L genes were deleted from the Hsp70 BAC 92G8-K/N 8.32 C-2 by homologous recombination using a BAC-recombineering protocol (Warming et al., 2005). A PCR product containing the *galK* gene flanked by two 48-bp homology boxes was used to replace the 8-kb target region with the *galK* gene. The primers used for PCR were 5′-GTGACAGGGCGAGACTGTCTCTCAAAACACACACACACACACACACCCTGTTGACAAT-3′ and 5′-CCTATGCAGACCCTACTGACCCCCAAATAAAGGAATAAAAGGCATCACTCAGCACTGTCC-3′. The *galK* gene was then deleted using a 100-bp DNA sequence corresponding to two 50-bp homology boxes flanking the inserted *galK* gene on the Hsp70 BAC. The restriction enzyme banding patterns for selected BAC clones were examined to ensure the correct deletion and BAC organization, using comparisons with the predicted digestion patterns generated by the Gene Construction kit software (Textco BioSoftware).

Microscopy and data analysis

3D optical-section datasets of fixed cells were collected using a 60× 1.4 NA objective on an inverted light microscope (IMT-2; Olympus) equipped with a slow scan (Photometrics), a cooled charge-coupled device camera unit (CE200A; Photometrics), motorized filter wheels, and a microstepping motor for z focus, all driven by the Resolve 3D software data collection program (Applied Precision) running on an SGI 4D/35TG. This system duplicates one built by D.A. Agard and J.W. Sedat and has been described previously in depth (Hiraoka et al., 1991). Alternatively, for data presented in Figs. 2 B, 3 C, 4 A (RNA FISH), 5, S1, and S2 (cadmium treatment), a deconvolution microscope system (Personal Deltavision; Applied Precision) was used with a 60× 1.4 NA lens. Deconvolution used an enhanced ratio, iterative constrained algorithm (Agard et al., 1989).

XY and Z optical displacement between different filter sets was determined experimentally using fluorescent microspheres (Tetraspeck; Invitrogen). Corrections for optical displacement and image scaling were performed with ImageJ (National Institutes of Health) open source software.

For RNA FISH quantitative measurements, all operations were performed with ImageJ software. Deconvolved image stacks were cropped to a single cell, and 16-bit z projections were calculated by summing intensities. The RNA FISH signal area was defined automatically by thresholding the images using the Otsu thresholding 16-bit function. The integrated signal intensity and the areas in square micrometers were measured in the defined area. RNA FISH signal densities were calculated by dividing the integrated intensity by the area measured in square micrometers. Figures were prepared using Photoshop and Illustrator software (Adobe).

Online supplemental material

Fig. S1 compares localization of Hsp70 nascent transcripts with transcripts from other genes on BACs. Fig. S2 shows no speckle association after cadmium Hsp70 gene induction. Table S1 shows statistical details for experimental comparisons including cell numbers, SEMs, and p-values. Online supplemental material is available at http://www.jcb.org/cgi/content/full/jcb.201004041/DC1.

This work was supported by grant GM58460 from the National Institute of General Medical Sciences awarded to A.S. Belmont.

Submitted: 08 April 2010
Accepted: 11 October 2010

References

Agard, D.A., Y. Hiraoka, P. Shaw, and J.W. Sedat. 1989. Fluorescence microscopy in three dimensions. *Methods Cell Biol.* 30:353–377. doi:10.1016/S0091-679X(08)60986-3

Chaumeil, J., I. Okamoto, and E. Heard. 2003. X-chromosome inactivation in mouse embryonic stem cells: analysis of histone modifications and transcriptional activity using immunofluorescence and FISH. *Methods Enzymol.* 376:405–419. doi:10.1016/S0076-6879(03)76027-3

Cmarko, D., P.J. Verschure, T.E. Martin, M.E. Dahmus, S. Krause, X.D. Fu, R. van Driel, and S. Fakan. 1999. Ultrastructural analysis of transcription and splicing in the cell nucleus after bromo-UTP microinjection. *Mol. Biol. Cell.* 10:211–223.

Cremer, T., and C. Cremer. 2001. Chromosome territories, nuclear architecture and gene regulation in mammalian cells. *Nat. Rev. Genet.* 2:292–301. doi:10.1038/35066075

Fakan, S., and P. Nobis. 1978. Ultrastructural localization of transcription sites and of RNA distribution during the cell cycle of synchronized CHO cells. *Exp. Cell Res.* 113:327–337. doi:10.1016/0014-4827(78)90373-7

Hall, L.L., K.P. Smith, M. Byron, and J.B. Lawrence. 2006. Molecular anatomy of a speckle. *Anat. Rec. A Discov. Mol. Cell. Evol. Biol.* 288:664–675.

Hiraoka, Y., J.R. Swedlow, M.R. Paddy, D.A. Agard, and J.W. Sedat. 1991. Three-dimensional multiple-wavelength fluorescence microscopy for the structural analysis of biological phenomena. *Semin. Cell Biol.* 2:153–165.

Holt, I., S. Mittal, D. Furling, G.S. Butler-Browne, J.D. Brook, and G.E. Morris. 2007. Defective mRNA in myotonic dystrophy accumulates at the periphery of nuclear splicing speckles. *Genes Cells.* 12:1035–1048. doi:10.1111/j.1365-2443.2007.01112.x

Hu, Y., I. Kireev, M.J. Plutz, N. Ashourian, and A.S. Belmont. 2009. Large-scale chromatin structure of inducible genes: transcription on a condensed, linear template. *J. Cell Biol.* 185:87–100. doi:10.1083/jcb.200809196

Jolly, C., C. Vourc'h, M. Robert-Nicoud, and R.I. Morimoto. 1999. Intron-independent association of splicing factors with active genes. *J. Cell Biol.* 145:1133–1143. doi:10.1083/jcb.145.6.1133

Kawata, K., R. Shimazaki, and S. Okabe. 2009. Comparison of gene expression profiles in HepG2 cells exposed to arsenic, cadmium, nickel, and three model carcinogens for investigating the mechanisms of metal carcinogenesis. *Environ. Mol. Mutagen.* 50:46–59. doi:10.1002/em.20438

Lallena, M.J., and I. Correas. 1997. Transcription-dependent redistribution of nuclear protein 4.1 to SC35-enriched nuclear domains. *J. Cell Sci.* 110:239–247.

Mintz, P.J., S.D. Patterson, A.F. Neuwald, C.S. Spahr, and D.L. Spector. 1999. Purification and biochemical characterization of interchromatin granule clusters. *EMBO J.* 18:4308–4320. doi:10.1093/emboj/18.15.4308

Nguyen, V.T., F. Giannoni, M.F. Dubois, S.J. Seo, M. Vigneron, C. Kédinger, and O. Bensaude. 1996. In vivo degradation of RNA polymerase II largest subunit triggered by alpha-amanitin. *Nucleic Acids Res.* 24:2924–2929. doi:10.1093/nar/24.15.2924

Nye, A.C. 2003. Effects of transcriptional activators on large-scale chromatin structure. PhD thesis. University of Illinois, Urbana-Champaign, IL. 154 pp.

Ohba, K., Y. Okawa, Y. Matsumoto, Y. Nakamura, and H. Ohta. 2007. Transcriptome analysis of rat kidney cells continuously exposed to cadmium using DNA microarray. *J. Toxicol. Sci.* 32:103–105. doi:10.2131/jts.32.103

O'Keefe, R.T., A. Mayeda, C.L. Sadowski, A.R. Krainer, and D.L. Spector. 1994. Disruption of pre-mRNA splicing in vivo results in reorganization of splicing factors. *J. Cell Biol.* 124:249–260. doi:10.1083/jcb.124.3.249

Shopland, L.S., C.V. Johnson, M. Byron, J. McNeil, and J.B. Lawrence. 2003. Clustering of multiple specific genes and gene-rich R-bands around SC-35 domains: evidence for local euchromatic neighborhoods. *J. Cell Biol.* 162:981–990. doi:10.1083/jcb.200303131

Smith, K.P., P.T. Moen, K.L. Wydner, J.R. Coleman, and J.B. Lawrence. 1999. Processing of endogenous pre-mRNAs in association with SC-35 domains is gene specific. *J. Cell Biol.* 144:617–629. doi:10.1083/jcb.144.4.617

Smith, K.P., M. Byron, C. Johnson, Y. Xing, and J.B. Lawrence. 2007. Defining early steps in mRNA transport: mutant mRNA in myotonic dystrophy type I is blocked at entry into SC-35 domains. *J. Cell Biol.* 178:951–964. doi:10.1083/jcb.200706048

Spector, D.L., W.H. Schrier, and H. Busch. 1983. Immunoelectron microscopic localization of snRNPs. *Biol. Cell.* 49:1–10.

Thiry, M. 1995. The interchromatin granules. *Histol. Histopathol.* 10:1035–1045.

Tumbar, T., G. Sudlow, and A.S. Belmont. 1999. Large-scale chromatin unfolding and remodeling induced by VP16 acidic activation domain. *J. Cell Biol.* 145:1341–1354. doi:10.1083/jcb.145.7.1341

Wansink, D.G., W. Schul, I. van der Kraan, B. van Steensel, R. van Driel, and L. de Jong. 1993. Fluorescent labeling of nascent RNA reveals transcription by RNA polymerase II in domains scattered throughout the nucleus. *J. Cell Biol.* 122:283–293. doi:10.1083/jcb.122.2.283

Warming, S., N. Costantino, D.L. Court, N.A. Jenkins, and N.G. Copeland. 2005. Simple and highly efficient BAC recombineering using galK selection. *Nucleic Acids Res.* 33:e36. doi:10.1093/nar/gni035

Williams, G.T., and R.I. Morimoto. 1990. Maximal stress-induced transcription from the human HSP70 promoter requires interactions with the basal promoter elements independent of rotational alignment. *Mol. Cell. Biol.* 10:3125–3136.

Xing, Y., C.V. Johnson, P.T. Moen Jr., J.A. McNeil, and J. Lawrence. 1995. Nonrandom gene organization: structural arrangements of specific pre-mRNA transcription and splicing with SC-35 domains. *J. Cell Biol.* 131:1635–1647. doi:10.1083/jcb.131.6.1635